



HAL
open science

S-Adenosyl-N-decyl-aminoethyl, a Potent Bisubstrate Inhibitor of Mycobacterium tuberculosis Mycolic Acid Methyltransferases

Julien Vaubourgeix, Fabienne Bardou, Fanny Boissier, Sylviane Julien, Patricia Constant, Olivier Ploux, Mamadou Daffé, Annaïk Quémard, Lionel Mourey

► **To cite this version:**

Julien Vaubourgeix, Fabienne Bardou, Fanny Boissier, Sylviane Julien, Patricia Constant, et al.. S-Adenosyl-N-decyl-aminoethyl, a Potent Bisubstrate Inhibitor of Mycobacterium tuberculosis Mycolic Acid Methyltransferases. *Journal of Biological Chemistry*, 2009, 284, pp.19321 - 19330. 10.1074/jbc.m809599200 . hal-03003382

HAL Id: hal-03003382

<https://hal.science/hal-03003382>

Submitted on 13 Nov 2020

HAL is a multi-disciplinary open access archive for the deposit and dissemination of scientific research documents, whether they are published or not. The documents may come from teaching and research institutions in France or abroad, or from public or private research centers.

L'archive ouverte pluridisciplinaire **HAL**, est destinée au dépôt et à la diffusion de documents scientifiques de niveau recherche, publiés ou non, émanant des établissements d'enseignement et de recherche français ou étrangers, des laboratoires publics ou privés.

S-Adenosyl-N-decyl-aminoethyl, a Potent Bisubstrate Inhibitor of *Mycobacterium tuberculosis* Mycolic Acid Methyltransferases[§]

Received for publication, December 19, 2008, and in revised form, March 26, 2009. Published, JBC Papers in Press, May 13, 2009, DOI 10.1074/jbc.M809599200

Julien Vaubourgeix^{†§}, Fabienne Bardou^{†§}, Fanny Boissier^{†§1}, Sylviane Julien^{†§}, Patricia Constant^{†§}, Olivier Ploux[¶], Mamadou Daffé^{†§}, Annaïk Quémard^{†§2}, and Lionel Mourey^{†§3}

From [†]CNRS, Institut de Pharmacologie et de Biologie Structurale, Département Mécanismes Moléculaires des Infections Mycobactériennes, 205 Route de Narbonne, F-31077 Toulouse, the [§]Université de Toulouse, Université Paul Sabatier, Institut de Pharmacologie et de Biologie Structurale, F-31077 Toulouse, and the [¶]Laboratoire de Biochimie des Micro-organismes: Enzymologie, Métabolisme, et Antibiotiques, Ecole Nationale Supérieure de Chimie de Paris, CNRS UMR 7573, F-75231 Paris, France

S-Adenosylmethionine-dependent methyltransferases (AdoMet-MTs) constitute a large family of enzymes specifically transferring a methyl group to a range of biologically active molecules. *Mycobacterium tuberculosis* produces a set of paralogous AdoMet-MTs responsible for introducing key chemical modifications at defined positions of mycolic acids, which are essential and specific components of the mycobacterial cell envelope. We investigated the inhibition of these mycolic acid methyltransferases (MA-MTs) by structural analogs of the AdoMet cofactor. We found that S-adenosyl-N-decyl-aminoethyl, a molecule in which the amino acid moiety of AdoMet is substituted by a lipid chain, inhibited MA-MTs from *Mycobacterium smegmatis* and *M. tuberculosis* strains, both *in vitro* and *in vivo*, with IC₅₀ values in the submicromolar range. By contrast, S-adenosylhomocysteine, the demethylated reaction product, and sinefungin, a general AdoMet-MT inhibitor, did not inhibit MA-MTs. The interaction between Hma (MmaA4), which is strictly required for the biosynthesis of oxygenated mycolic acids in *M. tuberculosis*, and the three cofactor analogs was investigated by x-ray crystallography. The high resolution crystal structures obtained illustrate the bisubstrate nature of S-adenosyl-N-decyl-aminoethyl and provide insight into its mode of action in the inhibition of MA-MTs. This study has potential implications for the design of new drugs effective against multidrug-resistant and persistent tubercle bacilli.

One-third of the world population is infected with the tubercle bacillus, *Mycobacterium tuberculosis*, and tuberculosis kills one person every 20 s. The inhaled pathogenic bacilli are taken up by phagocytosis by pulmonary macrophages, which, together with lymphocytes and dendritic cells, form granulomas. The bacilli persist in the granuloma until their reactivation, dissemination into the lungs, and the triggering of disease. The natural resistance of persistent tubercle bacilli to drugs and the emergence of multidrug-resistant and extensively drug-re-

sistant *M. tuberculosis* strains are two main concerns in the treatment of the disease. A survey carried out by the Centers for Disease Control and Prevention and the World Health Organization between 2000 and 2004 reported that 20% of 17,690 *M. tuberculosis* isolates from 49 countries were multidrug-resistant, and 2% were extensively drug-resistant (1). The development of new drugs effective against persistent and drug-resistant bacilli has therefore become a priority.

The thick lipid-rich envelope of the *Mycobacterium* genus is characterized by the presence of mycolic acids (MAs),⁴ very long chain (C₆₀–C₉₀) α -alkylated β -hydroxylated fatty acids (2). MAs are the major components of the mycomembrane (3, 4) lipid bilayer, which plays a key role in both the architecture and permeability of the mycobacterial envelope. The MA biosynthetic pathway is essential for mycobacterial survival. MAs are generated by Claisen condensation between two fatty acyl chains as follows: the very long meromycoloyl chain (C₄₀–C₆₀) and a shorter saturated chain (C₂₂–C₂₆) (2). The different types of MAs are defined by the presence of decorations introduced at proximal and distal positions of the meromycolic chain (Fig. 1A) by a family of paralogous S-adenosylmethionine-dependent methyltransferases (AdoMet-MTs), the mycolic acid methyltransferases (MA-MTs). These chemical modifications are known to be important for the pathogenicity, virulence, and persistence of *M. tuberculosis*. For example, the *cis*-cyclopropane introduced at the proximal position of α -MAs by PcaA has an impact on the persistence of the tubercle bacillus within infected organisms (5). Furthermore, the keto and methoxy groups, with a vicinal methyl ramification at the distal position of oxygenated MAs, play a role in *M. tuberculosis* virulence in the mouse model of infection (6) and have recently been reported to be involved in host-pathogen interplay. Indeed, oxygenated MAs have been shown to modulate IL-12p40 production by macrophages (7) and to trigger the *in vitro* differentiation of monocyte-derived macrophages into foamy macrophages, which house the bacillus in a dormant state, within granulomas (8). Oxygenated MA biosynthesis requires the

[§] The on-line version of this article (available at <http://www.jbc.org>) contains supplemental Figs. S1–S3 and Table 1.

¹ Present address: Institut de Biochimie et Génétique Cellulaires, UMR 5095 CNRS-Université Victor Segalen Bordeaux 2, 33077 Bordeaux Cedex, France.

² To whom correspondence may be addressed. Tel.: 33-561-175-576; Fax: 33-561-175-994; E-mail: annaik.quemard@ipbs.fr.

³ To whom correspondence may be addressed. Tel.: 33-561-175-436; Fax: 33-561-175-994; E-mail: lionel.mourey@ipbs.fr.

⁴ The abbreviations used are: MA, mycolic acid; CFAS, cyclopropane fatty acid synthase; CTAB, cetyltrimethylammonium bromide; DMSO, dimethyl sulfoxide; MIC, minimum inhibitory concentration; MA-MT, mycolic acid methyltransferase; SADAE, S-adenosyl-N-decyl-aminoethyl; AdoMet, S-adenosyl-L-methionine; AdoMet-MT, S-adenosylmethionine-dependent methyltransferase; AdoHcy, S-adenosyl-L-homocysteine; MES, 4-morpholineethanesulfonic acid.

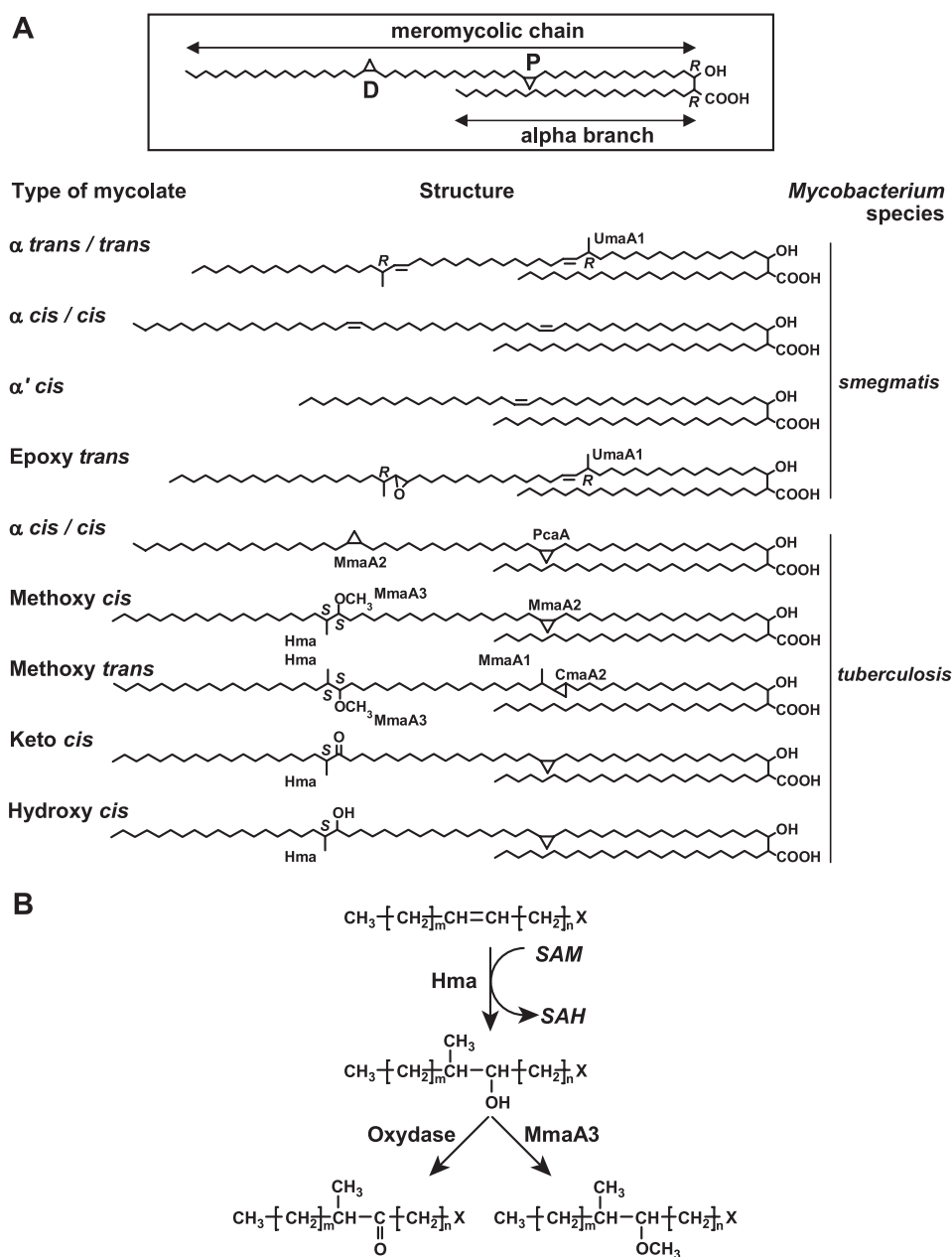


FIGURE 1. A, structures of MAs from *M. tuberculosis* and *M. smegmatis*. D, distal position; P, proximal position. Enzymes involved in the introduction of decorations on the meromycolic chain are indicated. B, proposed reaction scheme for the introduction of oxygenated groups. $m = 17, 19$; n , unknown; X, unknown carrier.

Hma (MmaA4) methyltransferase (Fig. 1B), as demonstrated by the absence of the oxygenated form in an *M. tuberculosis hma* knock-out mutant (6, 9). These results suggest that the enzymes responsible for adding the decorations to MAs, including oxygenated groups in particular, may be relevant pharmacological targets for the development of new antituberculous drugs (10).

Based on the essential role played by MA-MTs in the pathophysiology of tuberculosis, several studies have investigated the possible inhibition of this family of enzymes. A recent study revealed that the antituberculous drug thiacetazone and its chemical analogs inhibited MA cyclopropanation at concentrations in the micromolar range (11). Another study, based on mixtures of crude extracts of heat-inactivated mycobacteria and recombinant *Escherichia coli* overproduc-

ing MA-MTs, suggested that the incorporation of [^3H]AdoMet into growing meromycolic chains is inhibited by a high concentration (1 mg/ml, *i.e.* 2.6 mM) of *S*-adenosyl-L-homocysteine (AdoHcy) or sinefungin (12), the demethylated reaction product and a natural structural analog of AdoMet, respectively (Fig. 2). By contrast, AdoHcy and sinefungin are strong inhibitors of other AdoMet-MTs *in vitro*, including the cyclopropane fatty-acid synthase (CFAS) from *E. coli* (K_i of 30 and 0.22 μM , respectively) (13, 14). However, they are active only against the isolated enzyme, whereas *S*-adenosyl-*N*-decyl-aminoethyl (SADAE), a molecule in which the amino acid moiety of AdoMet is substituted by a lipid chain (Fig. 2), is active against CFAS both *in vitro* ($K_{i,\text{app}} = 6 \mu\text{M}$) and *in vivo* (complete inhibition at 150 μM) (15). The broad screening of possible inhibitors of MA-MTs with an *in vitro* mini-assay poses a major challenge, as these enzymes most likely use very long meromycolic chains as substrates. In this context, the similarity between CFAS and Hma in terms of their sequences (31% sequence identity) and substrates may be useful, as it suggests that SADAE may inhibit MA-MTs (15).

We report here our investigations of the interactions between Hma and SADAE, as compared with those between Hma and AdoHcy or sinefungin, and the potential impact of these interactions on the activities of Hma and other MA-MTs and mycobacterial growth. Our high resolution crystallographic charac-

terization of the Hma-SADAE interaction illustrates the bisubstrate nature of the ligand, which is strongly correlated with its strong inhibitory properties.

MATERIALS AND METHODS

Strains and Cultures—*M. tuberculosis* H37Rv was grown at 37 °C in Middlebrook 7H9 broth (Difco) supplemented with 0.2% (w/v) glycerol. *Mycobacterium smegmatis* mc²155/pMV261 and *M. smegmatis* mc²155/pMV261::hma (*mmaA4*, *Rv0642c*) strains were grown in the same medium supplemented with 10 $\mu\text{g/ml}$ kanamycin and, in some cases, albumin/dextrose/catalase. These recombinant strains were prepared as described previously (16).

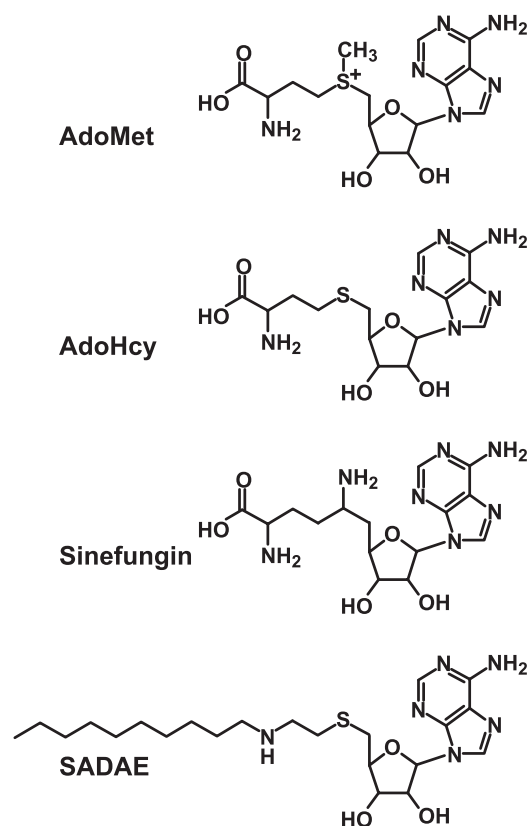


FIGURE 2. Structure of AdoMet and of the AdoHcy, sinefungin, and SADAE analogs.

Preparation of Cell Wall Extracts—Freshly grown bacteria were washed with 10 mM potassium phosphate buffer, pH 7.0, and resuspended in 50 mM potassium phosphate buffer, pH 7.0, plus 3 mM β -mercaptoethanol (buffer A). Bacteria were lysed by cell disruption, by two passages through a One-shot Cell Disrupter (Constant Systems Ltd.) at 0.8 kbar. The crude extracts were centrifuged for 15 min at $3,000 \times g$ and at 4 °C. The very dense layer at the surface of the supernatant, consisting of cell wall and membrane fragments (17), was removed, resuspended in buffer A, and homogenized with a syringe (needle size 0.7 \times 30 mm). The protein concentration of the extracts was determined with the DC method (Bio-Rad) for insoluble proteins, after denaturation of the proteins by boiling in 0.5 N NaOH at 100 °C for 10 min.

Evaluation of Ability of AdoMet Analogs to Inhibit MA Biosynthesis in Vitro—MA biosynthesis was assayed *in vitro* in a reaction medium containing 100 mM potassium phosphate buffer, pH 7.0, 3 mM $MgCl_2$, 7 mM $KHCO_3$, 7 mM ATP, 0.7 mM CoASH, and 500 μg of cell wall extract proteins in a total volume of 750 μl . Mixtures were first incubated in the presence or absence of AdoMet analogs (*i.e.* SADAE (10 μM), dissolved in dimethyl sulfoxide (DMSO) such that the maximum final solvent concentration in the reaction medium was 5% (v/v); AdoHcy (1 mM) and sinefungin (3 mM), evaluated either with or without DMSO) for 15 min at 37 °C, and we then added 50 μM of either [$1-^{14}C$]acetate for MA biosynthesis assays or [$CH_3-^{14}C$]AdoMet for MA-MT activity assays. Reaction mixtures were incubated at 37 °C for 60 min; the reactions were stopped

by saponification, and the MA profiles were analyzed by TLC (see below).

The apparent IC_{50} value of SADAE was determined by measuring the rate of MA biosynthesis in the presence of various concentrations of inhibitor (from 10 pM to 10 μM), using the same procedure as that described above, and calculated by fitting the data by nonlinear regression using the program GraphPad Prism 4.02.

[$1-^{14}C$]Acetate (specific activity, 56.60 mCi/mmol) and [$CH_3-^{14}C$]AdoMet (specific activity, 50.43 mCi/mmol) were purchased from PerkinElmer Life Sciences. Sinefungin ($M_r = 381.4$ g/mol) and AdoHcy ($M_r = 384.4$ g/mol) were obtained from Sigma, and SADAE ($M_r = 466.65$ g/mol) was obtained from the Institut de Chimie des Substances Naturelles (Gif sur Yvette, France).

Evaluation of the *in Vivo* Effects of SADAE on MA Biosynthesis—SADAE (50 and 90 μM) was added to broth cultures of *M. smegmatis* in the exponential growth phase. The cultures were then incubated at 37 °C for 90 min before the addition of 6.8 μM [$1-^{14}C$]acetate. Cells were incubated for 3 or 6 h and then harvested. For *M. tuberculosis* cultures, also in the exponential growth phase, SADAE was added at concentrations of 25, 50, and 90 μM . Cultures were incubated at 37 °C for 7 h before the addition of [$1-^{14}C$]acetate and then for a further 24 h before the harvesting of whole cells for MA content characterization.

Extraction and Analysis of MAs—Reaction media containing cell wall extracts or harvested whole bacteria were saponified by incubation with a mixture of 40% KOH (w/v)/methoxyethanol (1:7) for 3 h at 110 °C in a screw-capped tube (18). The suspensions were acidified by adding an equal volume of 20% H_2SO_4 , and fatty acids were extracted with diethyl ether. The neosynthesized and radiolabeled MAs were methylated and analyzed by TLC on Silica Gel 60 (Macherey-Nagel) run in dichloromethane for *M. smegmatis* strains and in petroleum ether/diethyl ether (9:1) (five runs) for *M. tuberculosis* (18), followed by phosphorimaging (Variable Mode Imager Typhoon TRIO, Amersham Biosciences). α -MAs were purified by preparative TLC on Silica Gel 60, and fractionated on $AgNO_3$ -impregnated silica gel TLC plates developed with dichloromethane (9, 19). The total labeled and unlabeled lipids in the extracts were visualized by spraying with molybdophosphoric acid (10% in ethanol) and charring. The radiolabeled spots were identified based on the R_f values of the fatty and mycolic acids visualized by the latter method and by comparison with previous data (16, 19).

Inhibition of Mycobacterial Growth—The susceptibility of *M. smegmatis* strains or of *M. tuberculosis* H37Rv to SADAE was evaluated by determining the minimum inhibitory concentration (MIC). We used a colorimetric microassay based on the reduction of 3-(4,5-dimethylthiazol-2-yl)-2,5-diphenyltetrazolium bromide (Sigma) to formazan by metabolically active cells (20–22). Briefly, serial 2-fold dilutions of the inhibitor were prepared in 100 μl of Middlebrook 7H9 broth base (Difco) and dispensed into 96-well microtiter plates, and to each well we added 100 μl of *M. tuberculosis* or *M. smegmatis* suspension (diluted in 7H9 broth to an A_{600} of 0.02). Plates were incubated for 6 days at 37 °C, and 3-(4,5-dimethylthiazol-2-yl)-2,5-diphenyltetrazolium bromide was added (50 μl of a 1 mg/ml solu-

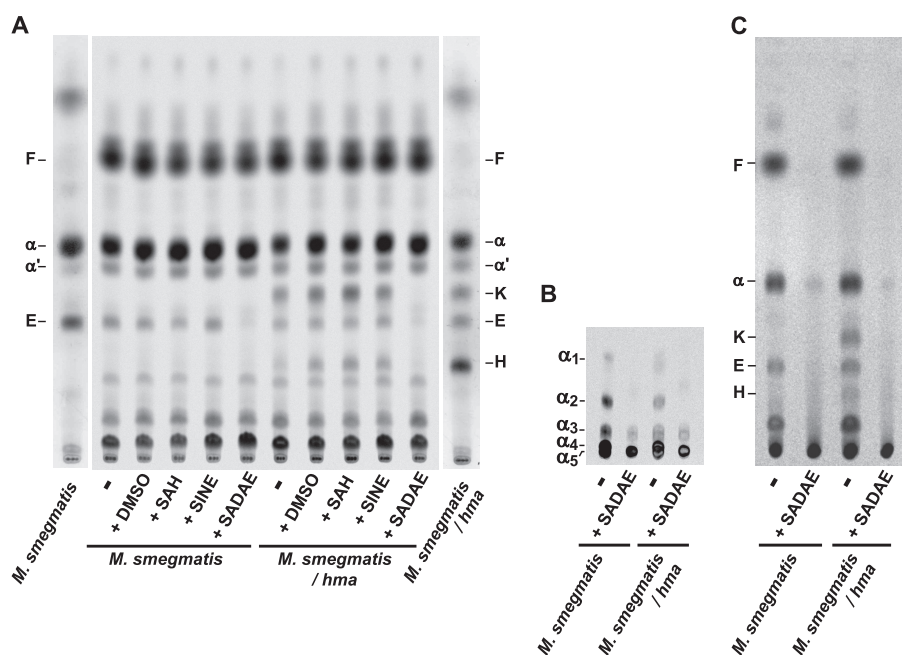


FIGURE 3. Effect of AdoMet analogs on MA biosynthesis and MA-MT activities *in vitro*. A, MA biosynthesis assays with *M. smegmatis*/pMV261 and *M. smegmatis*/pMV261::*hma* cell wall extracts and AdoHcy (1 mM), sinefungin (3 mM), or SADAE (10 μ M). Neosynthesized MAs were labeled by incubation with [14 C]acetate. Nonradiolabeled reference lipids were visualized by spraying molybdophosphoric acid (left and right lanes). B, [14 C]acetate-labeled α -MA methyl esters were scraped off the plate shown in A and separated by TLC on AgNO₃-impregnated plates. C, MA-MT activity assays with [14 C]AdoMet labeling. All TLC runs were performed with dichloromethane, and radiolabeled spots were detected by phosphorimaging and identified by comparison of their R_f with those of known lipids. F, fatty acid methyl esters; K, keto-; E, epoxy-; H, hydroxy-MA methyl esters. α_1 , *cis,trans*- or *cis,cis*-dicyclopropanic; α_2 , *cis*-cyclopropanic,*trans*-ethylenic; α_3 , *cis*-cyclopropanic,*cis*-ethylenic; α_4 , *cis,trans*-diethylenic; α_5 , *cis,cis*-diethylenic MA methyl esters.

tion). Plates were incubated for a further 24 h, and solubilization buffer (dimethylformamide/SDS 20% (w/v), 1:2) was added to each well. Absorbance was measured at 570 nm. The MIC was determined as the lowest concentration of SADAE yielding 100% inhibition of bacterial growth (the absorbance value obtained for untreated bacilli was taken as a growth control). Ethambutol- and isoniazid-treated cultures were used as positive controls.

X-ray Crystallography of Complexes of Hma with AdoMet Analogs—Crystals of apo-Hma were obtained from the purified His₆-tagged protein, as described previously (16). Crystals of the complex with AdoHcy were prepared by cocrystallization in the presence of 2 mM cofactor product. The crystals were cryo-cooled in a stream of nitrogen gas at 100 K after immersion for 3 min in the crystallization solution supplemented with 20% (v/v) glycerol. For preparation of the complex with sinefungin, crystals of the apo-form were soaked in a solution containing both the cryoprotectant and 50 mM sinefungin for 2 min. The complex with SADAE was prepared by soaking crystals of the apo-form three times in freshly prepared drops of 5 mM SADAE in crystallization conditions and 5% (v/v) DMSO, for a total soaking time of 15 min. A fourth soaking was then carried out during 3 min in a drop containing the same solution supplemented with 20% glycerol. All diffraction data were collected at multistation beam-line ID14 of the European Synchrotron Radiation Facility (Grenoble, France).

The CCP4 suite (23), as implemented in the graphical user interface (24), was used for crystallographic calculations. X-ray diffraction data were processed with MOSFLM (25) and scaled

with SCALA (26). The structures of the complexes were solved, using the previously determined crystallographic coordinates of Hma in complex with AdoMet (16) (Protein Data Bank code 2FK8) and discarding non-protein atoms. All structures were constructed manually in σA weighted electron density maps (27), using Coot (28). Restrained refinements were obtained with the REFMAC5 program (29), using a bulk solvent correction based on the Babinet principle and minimizing a maximum likelihood target function. Solvent molecules were automatically added as neutral oxygen atoms with wARP (30) and Coot. Ligands were added at the end of refinement after water attribution. The coordinates of AdoHcy and sinefungin (adenosylornithine) were obtained from the Hetero-compound Information Center Uppsala (HIC-Up) (31). The energy-minimized coordinates and refinement library for SADAE were generated with the PRODRG server (32). TLS parameters were refined, using a single group for the whole molecule (33), resulting in a similar improvement of the R and R_{free} values.

Protein-ligand interactions were defined with HBPLUS (34). Figs. 7–9 were produced using PyMOL (35).

RESULTS

Action of AdoHcy, Sinefungin, and SADAE on MA Biosynthesis *In Vitro*—We first tested the effects of the three putative inhibitors on MA-MT activities in cell wall extracts of *M. smegmatis*/pMV261 and *M. smegmatis*/pMV261::*hma*. With these bacterial extracts, the *in vitro* biosynthesis of MAs can be followed in the presence of a radiolabeled marker, [14 C]acetate. The neosynthesized and radiolabeled MAs were extracted, methylated, and then analyzed by TLC and phosphorimaging. SADAE almost totally inhibited the biosynthesis of epoxy-MAs in *M. smegmatis*/pMV261 and that of epoxy-, keto-, and hydroxy-MAs in *M. smegmatis*/pMV261::*hma* (Fig. 3A), at a concentration similar to the K_i of CFAS, 10 μ M (15). By contrast, concentrations of the structural analogs AdoHcy and sinefungin 100–300 times higher than the effective concentration of SADAE had no significant impact on these metabolic pathways (Fig. 3A).

A potentially specific effect of SADAE on the various species of α -MAs was investigated further after separation on AgNO₃-impregnated TLC plates. Interestingly, in the treated cell wall extracts of both transformed and untransformed *M. smegmatis* strains, *cis,cis*-diethylenic α -MA (α_5) labeling essentially persisted (Fig. 3B), whereas the labeling of *cis,cis* or *cis,trans*-dicyclopropanic (α_1), *cis*-cyclopropanic,*trans*-ethylenic (α_2), and *cis,trans*-diethylenic (α_4) MAs was undetectable and that of the

cis-cyclopropanic, *cis*-ethylenic MA (α_3) was weaker (Fig. 3B and Fig. 1A). These data strongly suggest that SADAЕ interfered with the activity of MA-MTs. We tested this hypothesis by carrying out a similar experiment with $[\text{CH}_3\text{-}^{14}\text{C}]\text{AdoMet}$, which is specific for AdoMet-MT activity. In these conditions, only MAs bearing a cyclopropane (α -MA subpopulation in *M. smegmatis* (19)) or a methyl branch (oxygenated MAs or α_1 - to α_4 -MAs) were radiolabeled in untreated cell wall extracts because they incorporated ^{14}C -methyl groups (Fig. 3C). Radioactivity was also detected in methyl-branched fatty acids, corresponding to tuberculostearic acid (10-methylstearic acid) and its homolog 10-methylpalmitic acid (Fig. 3C and supplemental Fig. 1). As expected, almost no labeling of MAs or fatty acids was observed in the presence of SADAЕ (Fig. 3C).

The apparent IC_{50} value of SADAЕ was determined by measuring the rate of oxygenated MA biosynthesis over a large range of inhibitor concentrations. The IC_{50} values for keto-MA and for epoxy-MA synthesis were $0.065 \pm 0.013 \mu\text{M}$ ($0.031 \pm 0.006 \mu\text{g/ml}$) and $0.713 \pm 0.036 \mu\text{M}$ ($0.333 \pm 0.017 \mu\text{g/ml}$), respectively. The submicromolar IC_{50} values reflect the high potential of SADAЕ to inhibit MA-MTs.

SADAЕ Inhibits the Growth of *M. smegmatis* and *M. tuberculosis*—The failure of most antibiotics to permeate the exceptionally impermeable mycobacterial cell wall is a major cause of poor whole-cell potency and a lack of susceptibility to drugs in mycobacteria (36). We also assessed the impact of SADAЕ on the growth of mycobacterial species by determining MICs for *M. smegmatis*/pMV261, *M. smegmatis*/pMV261:*hma*, and *M. tuberculosis*. The mycobacterial cells were grown in microplates, and serial 2-fold dilutions of SADAЕ were added during the exponential growth phase. The final counts of bacteria were determined by measuring the metabolism of a tetrazolium salt into a colored compound, formazan, detected at 570 nm. Curves showed growth inhibition at similar concentrations for both *M. smegmatis* and *M. tuberculosis*, corresponding to MIC values of about $100 \mu\text{M}$ ($47 \mu\text{g/ml}$) (Fig. 4). Thus, SADAЕ is able to reach targets within the bacilli and to stop mycobacterial growth.

Action of SADAЕ on MA-MTs *in Vivo*—We investigated whether MA-MTs were particularly accessible to SADAЕ and could be considered among its targets *in vivo*, by evaluating the effect of this compound on the biosynthesis of MAs in intact mycobacteria. We first treated *M. smegmatis*/pMV261 and *M. smegmatis*/pMV261:*hma* cultures at ($100 \mu\text{M}$) or below ($50 \mu\text{M}$) the MIC, for 90 min, and then added $[1\text{-}^{14}\text{C}]\text{acetate}$. Cultures were incubated for 3 or 6 h, and the lipids were then extracted. TLC analysis showed that SADAЕ almost totally inhibited the biosynthesis of epoxy-, keto-, and hydroxy-MAs at the MIC (Fig. 5A and supplemental Fig. 2). We then carried out similar experiments on *M. tuberculosis*. Bacteria were treated with SADAЕ concentrations of $25\text{--}90 \mu\text{M}$ for 7 h, and were then labeled with $[1\text{-}^{14}\text{C}]\text{acetate}$ for 24 h (Fig. 5B). The biosynthesis of oxygenated MAs was strongly inhibited. Relative radiolabeling levels for these MAs were up to 86% lower than those in the absence of SADAЕ, whereas α -MA and regular size fatty acid levels remained stable (Fig. 5D).

We investigated the effects of SADAЕ treatment on the structure of α -MAs in more detail by purifying these com-

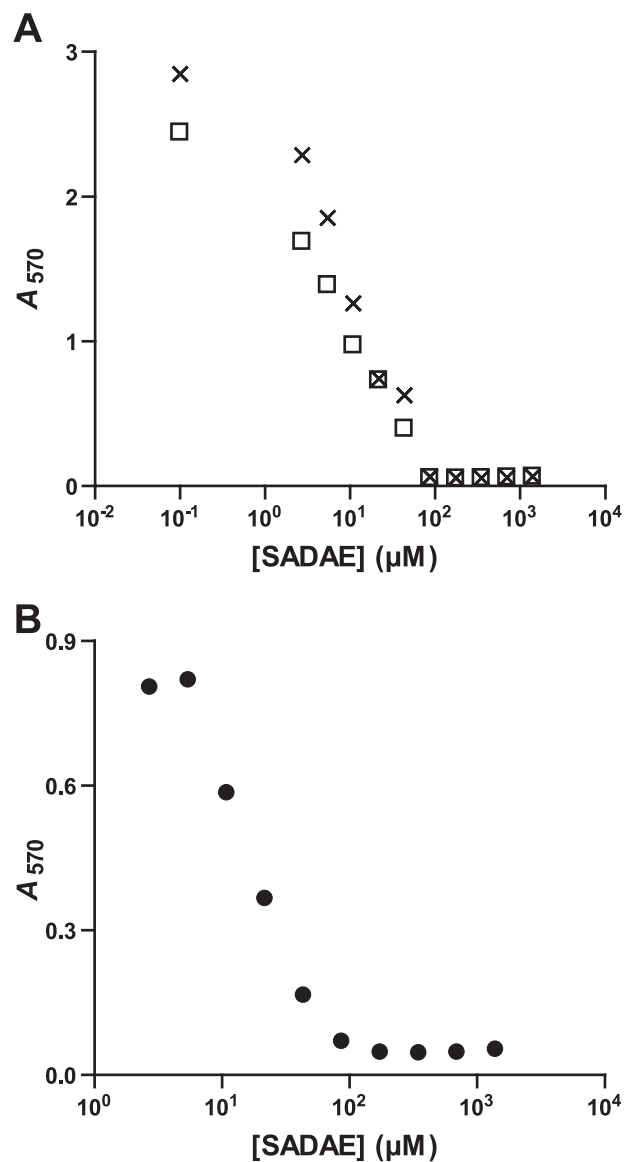


FIGURE 4. Determination of the MIC values of SADAЕ. A, *M. smegmatis*/pMV261 (crosses) and *M. smegmatis*/pMV261:*hma* (open squares). B, *M. tuberculosis*.

pounds and analyzing them by argentation TLC (Fig. 5C). Untreated *M. tuberculosis* produced dicyclopropanated MAs (α_1'), but the profile of compounds produced was radically changed by SADAЕ treatment. SADAЕ strongly inhibited the synthesis of α_1' -MAs (86% inhibition at $90 \mu\text{M}$) and induced the accumulation of several new species with a much smaller R_f (Fig. 5E). The migration of these compounds corresponded to that of mono- and di-ethylenic α -MAs (α_2' and α_3' , respectively) (9, 19). The appearance of unsaturated α -MAs probably results from the inhibition of PcaA and MmaA2, which introduce *cis*-cyclopropane rings into α_1' -MAs, and the inhibition of Hma and MmaA2/CmaA2, which catalyze the biosynthesis of *cis/trans*-cyclopropanated oxygenated MAs (Fig. 1). These data collectively demonstrate that SADAЕ also inhibits MA-MTs with cyclopropane synthase activity.

In conclusion, SADAЕ concentrations equivalent to the MIC inhibit MA-MTs *in vivo* in both *M. smegmatis* and *M. tuberculosis*.

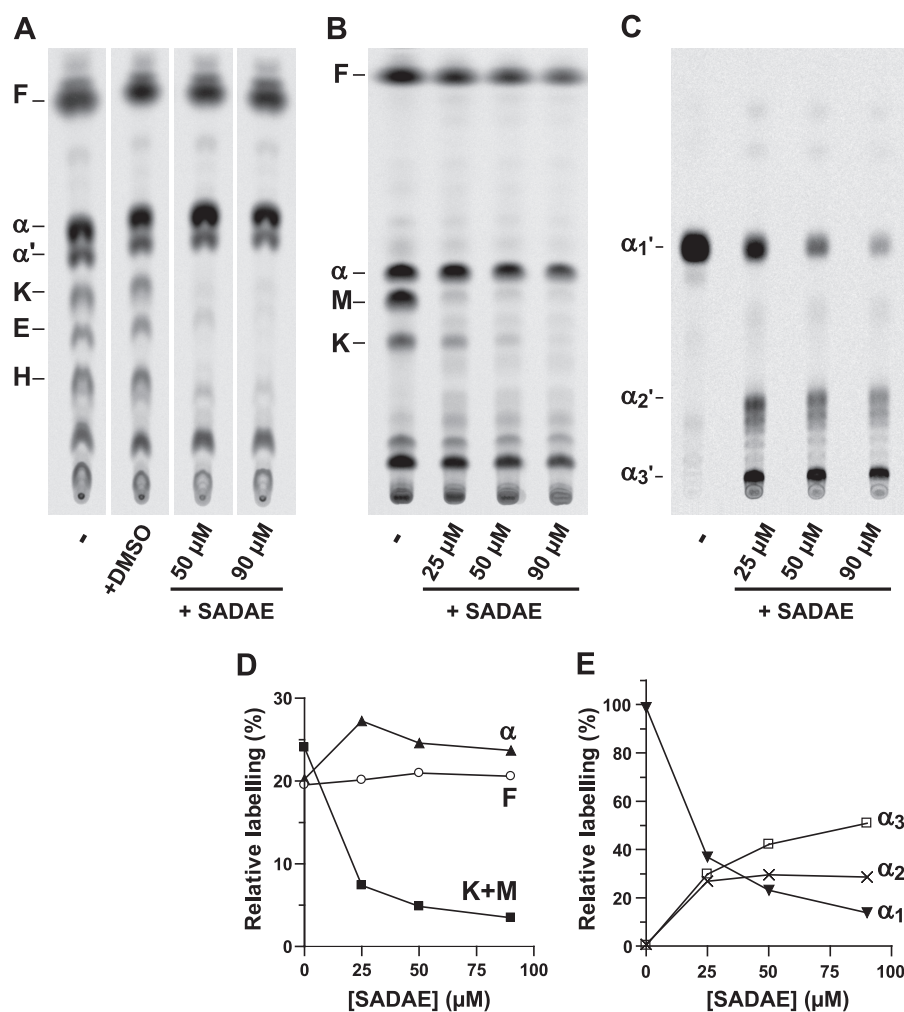


FIGURE 5. Inhibition of MA-MT activities *in vivo*. Bacteria in culture were treated with various concentrations of SADAE, and the neosynthesis of mycolic acids *in vivo* was followed by [^{14}C]acetate labeling. *A*, *M. smegmatis*/pMV261::h*ma*. Only points after 6 h of incubation are displayed for reasons of clarity; similar profiles were obtained after 3 h of incubation. *B* and *C*, *M. tuberculosis*. *C*, α -MA methyl esters scraped off the plate shown in *B* and separated by TLC on an AgNO_3 -impregnated silica gel plate. *D* and *E*, relative labeling intensities for the various molecular species assessed on plates *B* and *C*, respectively. All runs were performed with dichloromethane (*A* and *C*) or petroleum ether/diethyl ether (9:1) (five times) (*B*), and radiolabeled spots were detected by phosphorimaging. *F*, fatty acid methyl esters; *K*, keto-; *E*, epoxy-; *H*, hydroxy-; *M*, methoxy-MA methyl esters. α_1' , dicyclopropanated; α_2' , monoethylenic-monocyclopropanated; α_3' , diethylenic α -MA methyl esters.

For oxygenated groups, the activities of Hma in MA biosynthesis in *M. tuberculosis* and of uncharacterized enzymes in the synthesis of *M. smegmatis* epoxy-MAs were at least impaired, whereas the effects of SADAE on the activity of MmaA3, the MA-MT catalyzing the introduction of a methyl group downstream from the Hma reaction (Fig. 1*B*), remained unclear.

Determination and Comparison of the Three-dimensional Structures of Hma in Complex with AdoHcy, Sinefungin, and SADAE—We investigated the reasons for this unique effect of SADAE on MA-MT function not observed with AdoHcy and sinefungin by determining the high resolution crystal structure of the complexes formed between Hma and the three ligands. Crystals of His₆-tagged Hma prepared in 50 mM MES, 50 mM NaCl, pH 6.5, were grown from the purified protein, using various amounts of polyethylene glycol 3350 over a broad pH range, as reported previously (16). Complexes with the cofactor analogs were obtained either by cocrystallization or through

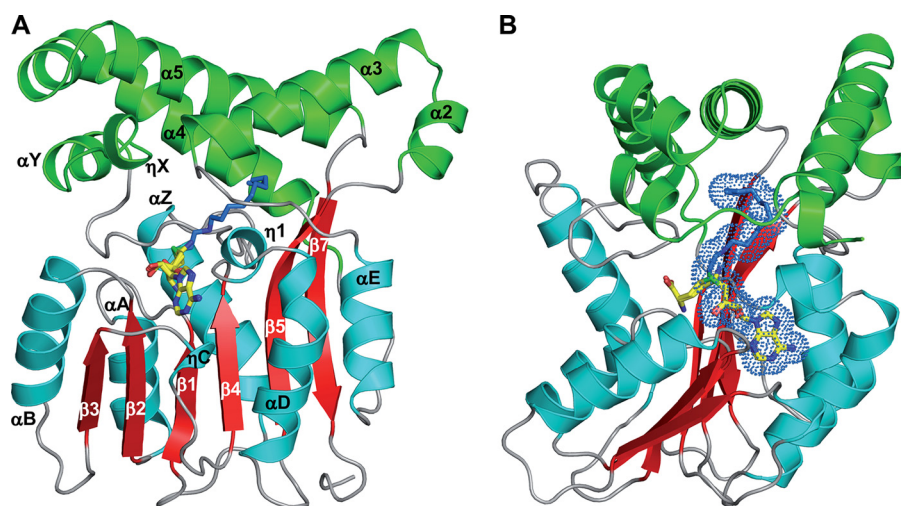
soaking experiments. SADAE is not directly soluble in water, and DMSO was therefore required for its solubilization, as for many organic compounds. We used concentrations of inhibitor no greater than 5 mM to minimize the final concentration of DMSO. At this concentration, a single soaking for a few minutes gave insufficient density for the ligand. By contrast, SADAE binding was achieved by iterative soakings, each time in a new drop. Complete data sets were collected for all three complexes, from single crystals at a maximum resolution of 2.2 to 2.35 Å. Initial model building was based on the known three-dimensional structure of Hma in complex with the cofactor substrate (16), taking into account only the protein atoms. Refinement was run smoothly. We first modified the protein, then introduced water molecules, and finally assigned the compounds whose position and orientation were obvious from the electron density maps (supplemental Fig. 3). Refinement statistics are summarized in Table 1. All structures have >91% of the residues in the most favored region of the Ramachandran plot and none in the disallowed region, as defined by PROCHECK (37).

The overall structure of the Hma protein in complexes with AdoHcy, sinefungin, and SADAE is very similar to that of Hma-AdoMet (16), giving root mean square deviation (r.m.s.d.)

values after superimposition of 0.5 Å/281 C- α atoms, 0.5 Å/281 C- α atoms, and 0.6 Å/270 C- α atoms for the complexes with AdoHcy, sinefungin and SADAE, respectively. All three structures display characteristic folding of residues 158–160 as 3_{10} helix η_1 (the secondary structure numbering used is from Ref. 16), a marker of AdoMet-MT-cofactor complex formation. As already reported for Hma-apo and Hma-AdoMet (16), there are missing residues at the N terminus, which starts at residue number 21 for AdoHcy and sinefungin, and residue 27 for SADAE. Residues 186–187 (within helix α_2), residues 263–264 (making a short connection between helices α_4 and α_5), and residue 301 at the C terminus are also missing in the Hma-SADAE complex (supplemental Fig. 3). It has previously been reported that helix α_B , encompassing residues 105–120, is translated along its axis toward the cofactor binding cleft upon AdoMet binding (16). In the three complexes described here, this helix occupies the same position as in Hma-apo. Thus, helix α_B seems to display dynamics of

TABLE 1
Data collection and refinement statistics

	Crystal		
	Hma-AdoHcy	Hma-sinefungin	Hma-SADAE
Data collection			
Beam line	ID14-2	ID14-1	ID14-4
Space group	P3 ₁ 21	P3 ₁ 21	P3 ₁ 21
Unit cell dimensions, Å	$a = b = 57.34, c = 203.98$	$a = b = 56.78, c = 202.79$	$a = b = 57.43, c = 205.08$
Resolution limits, ^a Å	28.7 to 2.2 (2.32 to 2.20)	27.3 to 2.3 (2.42 to 2.30)	20.0 to 2.35 (2.48 to 2.35)
No. of measured reflections	69,191 (9536)	91,988 (13,557)	73,932 (11,193)
No. of unique reflections	20,193 (2844)	17,694 (2532)	16,765 (2422)
Completeness, %	98.4 (97.8)	99.8 (100.0)	98.2 (99.4)
R_{sym} , %	4.7 (30.1)	6.2 (32.6)	4.6 (32.7)
$I/\sigma I$	9.1 (2.4)	8.1 (2.3)	10.1 (2.4)
B_{Wilson} , Å ²	44.1	43.8	60.2
Refinement statistics			
Resolution range, ^a Å	28.7 to 2.2 (2.26 to 2.20)	27.3 to 2.3 (2.36 to 2.30)	20.0 to 2.35 (2.41 to 2.35)
No. of residues/total expected ^b	281/318	281/318	270/318
Missing residues	tag, 4–20	tag, 4–20	tag, 4–26, 186–187, 263–264, 301
No. of protein atoms	2256	2235	2081
No. of water molecules	63	67	45
No. of ligand atoms	26	27	32
No. of heteroatoms	2345	2329	2158
No. of reflections work/test ^a	19,162/1031	16,737/897	15,905/849
Crystallographic R factor/ R_{free} ^a	0.202/0.250 (0.241/0.294)	0.183/0.229 (0.205/0.263)	0.211/0.243 (0.236/0.280)
r.m.s.d. bond lengths, Å	0.018	0.017	0.014
r.m.s.d. bond angles, °	1.674	1.558	1.439
r.m.s.d. planarity, Å	0.114	0.104	0.106
Mean temperature factor, Å ²			
Main chain ^c	56.7	55.6	87.0
Side chain ^c	58.4	56.8	86.2
Solvent	55.5	52.1	86.5
Ligand	55.3	46.7	88.7

^a The numbers in parentheses are for the highest resolution shell.^b Data were derived by taking into account the changes brought to the sequence.^c Full B factors are given, including the contribution of TLS parameters.**FIGURE 6. Three-dimensional structure of the complexes formed between Hma and AdoHcy, sinefungin, and SADAE.** *A*, ribbon representation of Hma (coordinates from the Hma-AdoHcy complex) showing helices and β -strands of the conserved AdoMet-MTs core in cyan and red, respectively. Helices of the MA-MT embellishment pattern are shown in green. The three ligands were superimposed and are shown as sticks with carbon atoms of the adenosine core in yellow and nitrogen, oxygen, and sulfur atoms in blue, red, and green, respectively. The carbon atoms of the decylaminoethyl group of SADAE are shown in navy. *B*, perpendicular view. The van der Waals surfaces of SADAE atoms are also depicted with dots.

unknown function. Other regions displaying structural variations (deviations exceeding r.m.s.d. values when in comparison with the structure of Hma-AdoMet) are confined to the N-terminal end, the $\alpha 2$ - $\alpha 3$ motif, and $\alpha 4$ - $\alpha 5$, all of which contribute to the embellishment pattern of MA-MTs.

Fine Description of the Complexes—The ligands used in this study bear a common adenosine core and specific non-nucleoside appendages in the C-5' position, the specific appendages of

AdoHcy and sinefungin at this position being similar (Fig. 2). AdoHcy and sinefungin bind to Hma at the same position and in a similar bent conformation as observed for Hma-AdoMet (16) and for other MA-MTs (38). Indeed, all three ligands are positioned on Hma with the ribose lying at the apex of the β -sheet contributing to the AdoMet-MT canonical fold, whereas the adenine is sandwiched on one side of the β -sheet, between the tip of strand $\beta 1$, helix $\eta 1$, and the loop between strand $\beta 3$ and helix ηC , with the amino acid portion pointing toward the N terminus of helix αA on the other side of the β -sheet (Fig. 6). The superimposition of AdoHcy and sinefungin with AdoMet in Hma complexes gave r.m.s.d. values of 0.2 Å for 26 and 25 common atoms, respectively. Specific hydrogen bonds and hydrophobic contacts between both the common adenosine core and the amino acid appendage and protein residues are mostly conserved (Fig. 7, *A* and *B*, and supplemental Table 1).

In the Hma-SADAE complex, the interactions of the adenine and sugar moieties with the protein are also conserved (Fig. 7*C* and supplemental Table 1), and the r.m.s.d. obtained after superimpo-

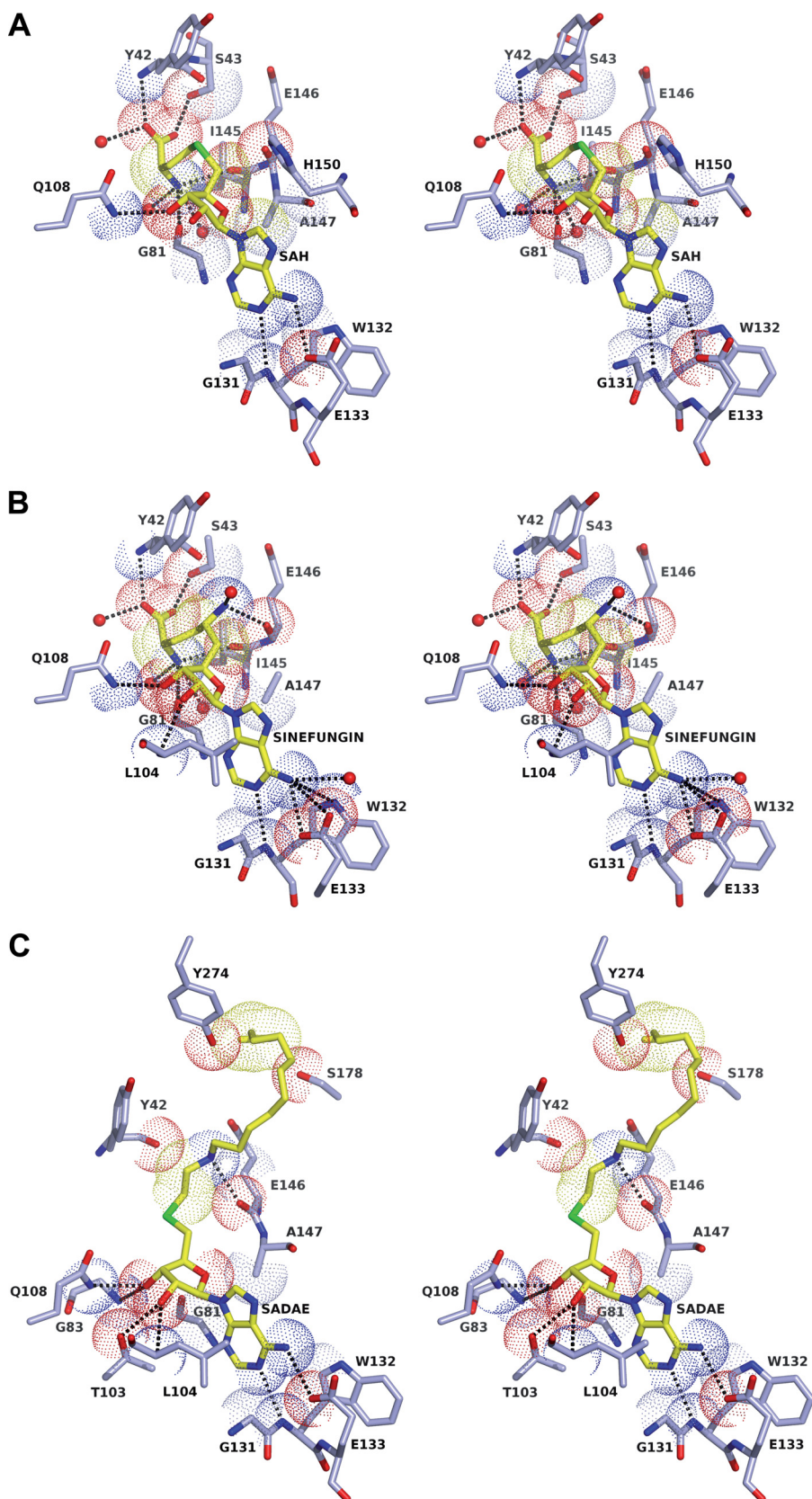


FIGURE 7. **Binding of AdoHcy, sinefungin, and SADAE to Hma.** Stereo image of the chemical environment of AdoHcy (A), sinefungin (B), and SADAE (C). The three ligands and the residues defining the corresponding binding sites in Hma are shown and labeled. Nitrogen, oxygen, and sulfur atoms are shown in blue, red, and green, respectively. Carbon atoms are shown in light blue for the protein and yellow for AdoHcy, sinefungin, and SADAE. The van der Waals surfaces of interacting atoms (listed in supplemental Table 1) are also shown. Water molecules are shown as red spheres. Hydrogen bonds are represented by black dotted lines.

sition with AdoMet is 0.12 Å for 19 common atoms. By contrast, the aliphatic tail, which is borne by the C-5' atom of SADAE, runs in the opposite direction to the amino acid counterparts of AdoMet/AdoHcy and sinefungin. The decylaminoethyl group points toward the center of the embellishment pattern of MA-MTs (Fig. 6), in a binding pocket delineated by residues Tyr-42 (between the N-terminal helices αY and αZ), Glu-146 (in the loop between strand $\beta 4$ and helix $\eta 1$), Glu-149 and His-150 (helix $\eta 1$), Ser-178 (strand $\beta 5$), Ile-204 (helix $\alpha 3$), Phe-209 (at the C terminus of helix $\alpha 3$), Leu-214 (in the loop between helices $\alpha 3$ and αE), Tyr-241 and Leu-245 (helix $\alpha 4$), and Tyr-274, Cys-278, and Phe-282 (helix $\alpha 5$). The lipophilic group of SADAE is tightly sequestered but nonetheless makes a few van der Waals/hydrophobic interactions with the protein, through carbon atoms located at both ends of the tail, and a single hydrogen bond between the nitrogen atom of the tail and the main chain oxygen atom of Glu-146 (Fig. 7C and supplemental Table 1). Two different conformations are found in equal proportions at the very tip (the last two carbon atoms) of the aliphatic chain of SADAE, indicating that its orientation is not restricted. As described at the end of the previous section, SADAE binding seems to induce perturbations in the embellishment pattern of MA-MTs, with electron density less well defined in some regions. Moreover, some protein residues are shifted when the ligand is present in the binding pocket. These residues correspond, in order of increasing displacement when compared with other structures, to Tyr-42 (0.7 Å), Tyr-274 (0.9 Å), His-150 (1.2 Å), Ile-204 (1.2 Å), and Phe-209 (1.5 Å). Local rearrangements in the immediate surroundings of SADAE also seem to be accompanied by small amplitude medium range effects on the loop between helices $\eta 1$ and αD , the N terminus of αD , the last two turns of $\alpha 3$, and the first two turns of $\alpha 5$.

The three-dimensional structure of Hma-SADAE shows that the lipid moiety binds in a U-shaped confor-

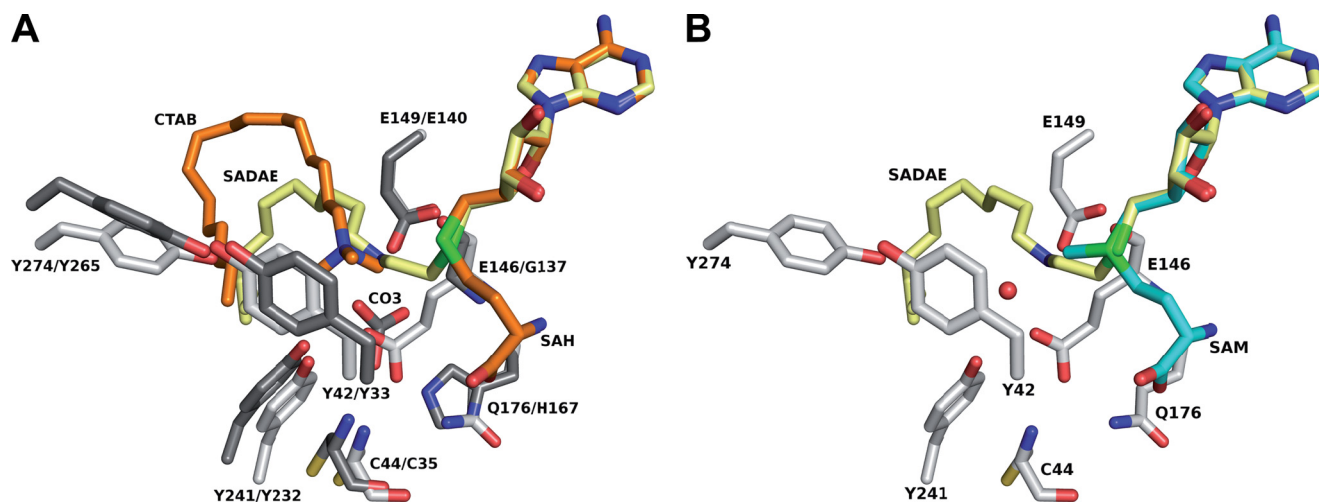


FIGURE 8. **Active-site architecture of MA-MTs.** A, chemical environment of SADAE in Hma and of AdoHcy and a cationic lipid, as observed in the structure of MmaA2-AdoHcy-CTAB (Protein Data Bank code 1TPY). B, superimposition of SADAE and AdoMet from the Hma-AdoMet complex (Protein Data Bank code 2FK8). Color code is as follows: Hma, light gray carbon atoms; MmaA2, dark gray carbon atoms; SADAE, yellow carbon atoms; AdoHcy and CTAB, orange carbon atoms; AdoMet, cyan carbon atoms. The Hma-AdoMet active site water molecule discussed in the text is represented as a red sphere. Residue numbering: Hma/MmaA2.

mation, with the 10-carbon alkyl chain partly superimposed on the alkyl chains of the two cationic detergents, didecyltrimethylammonium bromide and cetyltrimethylammonium bromide (CTAB), which have been crystallized with CmaA2 (38) and MmaA2, respectively, and were suggested to define the substrate-binding pocket (38) (Fig. 8A). The nitrogen atom of the 2-*N*-decylaminoethyl group of SADAE is found at approximately the same position as the positively charged quaternary nitrogen atom of CTAB/didecyltrimethylammonium bromide, with a distance between the two atoms (calculated on the basis of the nonoptimized C- α superimposition of the structures) of about 1.4 Å (Fig. 8A). However, the nitrogen atom of SADAE, which is likely to be mostly charged under our crystallization conditions (*i.e.* pH 6.5), most probably mimics the positively charged carbon atom of the high energy carbocation intermediate, as it is closer to the CE atom of the AdoMet methyl group and at good distance for the nucleophilic attack by the water molecule hydrogen-bonded to the carboxylate group of Glu-146 in the active site of the Hma-AdoMet complex (16) (Fig. 8B).

DISCUSSION

Two structural analogs of the AdoMet cofactor, its demethylated product AdoHcy and sinefungin, which has antibiotic activity, have been reported to inhibit prokaryotic and eukaryotic AdoMet-dependent methyltransferases (39–41) and the CFAS from *E. coli* (13, 14). Given their broad effect, we decided to evaluate the ability of these two molecules to inhibit MA-MTs, with the aim of rationally improving their potency and specificity. Both molecules interacted with the Hma MA-MT from *M. tuberculosis*, as shown by crystallography, but were found to have no significant effect on the biosynthesis of MAs *in vitro*.

By contrast, SADAE, in which the amino acid part of AdoMet analogs is replaced by 2-*N*-decylaminoethyl, strongly inhibited MA modification. This was demonstrated *in vitro*, using both the wild-type and a recombinant *M. smegmatis* strain into which the *M. tuberculosis hma* gene had been introduced. Our

data clearly revealed an absence of neosynthesis of the naturally occurring epoxy- and cyclopropanated or methyl-branched α -MAs, and of hydroxy- and keto-MAs, following the treatment of cell wall extracts from these strains with SADAE. Thus, SADAE can simultaneously target the whole range of enzymes responsible for introducing chemical groups at both the proximal and distal positions of these MAs. This action is similar to that of the antituberculous prodrug thiacetazone, although thiacetazone has been shown to target only the MA-MTs involved in MA cyclopropanation (11). SADAE also inhibited MA-MTs *in vivo* and stopped the growth of both *M. smegmatis* and *M. tuberculosis*. The concentrations almost totally inhibiting MA-MT activities *in vivo* correlate with the MIC values (100 μ M). Thus, the bacteriostatic effect of SADAE is linked to combined inhibition of the pool of MA-MTs within bacilli, including at least Hma, PcaA, MmaA2, and CmaA2 (Fig. 1A). The inactivation of a single MA-MT gene slows but does not abolish the *in vitro* multiplication of mycobacteria (6), but the total absence of chemical group introduction into the meromycolic chains may result in the death of the mycobacteria or, at least, an inability to divide. However, we cannot rule out the potential inhibition of other targets by SADAE.

The three-dimensional structure of the complex formed between Hma and SADAE shows that the ligand sits both in the cofactor-binding site and the putative substrate-binding pocket. More precisely, the adenosine moiety of SADAE exactly replaces that of the cofactor, whereas the lipid chain is deeply buried in the hydrophobic environment provided by the residues lining the substrate-binding pocket. Thus, the potent inhibition mediated by SADAE seems to be linked to its ability to compete with both the cofactor and the substrate. This finding is consistent with the inhibition kinetics of the *E. coli* CFAS enzyme, suggesting that SADAE behaves as a noncompetitive bisubstrate inhibitor able to bind to both cofactor- and substrate-binding sites, in which it competes with AdoMet for binding to the free enzyme and with lipids for binding to the

binary enzyme-cofactor complex (15). SADAЕ was a more effective inhibitor of MA-MTs ($0.1 < IC_{50} (\mu M) < 1$) than of *E. coli* CFAS ($IC_{50} = 10 \mu M$) (15) *in vitro*.

The bisubstrate nature of the SADAЕ inhibitor was unequivocally demonstrated for Hma through the structure of the complex between these two molecules. Given the strong conservation of the sequence and structure of the substrate-binding pocket, we anticipate that this effect might be generalized to all MA-MTs, thus accounting for the remarkable inhibition effect observed *in vivo* and *in vitro*. We and others have argued that the use of such a molecule, with pleiotropic effects on several MA-MTs, would greatly decrease the probability of bacilli developing a resistance phenotype (11, 16, 38) and would therefore be a good starting point for the development of a new antituberculous drug. Furthermore, MA-MTs contribute to the virulence and persistence of the tubercle bacillus (5, 6), and to pathogen-induced immunomodulation of the host (7, 8, 42). Thus, in addition to inhibiting bacterial multiplication, SADAЕ may represent a first step toward the design of antituberculous molecules that would allow the elimination of persistent bacilli. The stronger inhibition observed for SADAЕ than for AdoHcy or sinefungin probably derived from large favorable entropy, because of the hydrophobic effect forcing the lipophilic tail out of the solvent and into the hydrophobic substrate-binding cavity of MA-MTs. As recently suggested (43), a modest gain in the enthalpy contribution to the thermodynamic signature of the molecule could bring significant benefits in terms of binding affinity. Current works in our laboratory are dedicated to lead optimization of the adenosine core, using a fragment-based approach (44).

Acknowledgments—We thank Nawel Slama, Audrey Noguera, and Romain Galy for technical assistance. We thank Valérie Guillet, Laurent Maveyraud, and Samuel Tranier for assistance with data collection and the scientific staff of the European Synchrotron Radiation Facility (Grenoble, France) for excellent data collection facilities. We also thank Françoise Viala for help in preparing the figures.

REFERENCES

- Center for Disease Control and Prevention (2006) *MMWR Morb. Mortal Wkly Rep.* **55**, 301–305
- Marrakchi, H., Bardou, F., Lanéelle, M. A., and Daffé, M. (2008) in *The Mycobacterial Cell Envelope* (Daffé, M., and Reyrat, J. M., eds) pp. 41–62, American Society for Microbiology, Washington, D. C.
- Hoffmann, C., Leis, A., Niederweis, M., Pletzko, J. M., and Engelhardt, H. (2008) *Proc. Natl. Acad. Sci. U.S.A.* **105**, 3963–3967
- Zuber, B., Chami, M., Houssin, C., Dubochet, J., Griffiths, G., and Daffé, M. (2008) *J. Bacteriol.* **190**, 5672–5680
- Glickman, M. S., Cox, J. S., and Jacobs, W. R., Jr. (2000) *Mol. Cell* **5**, 717–727
- Dubnau, E., Chan, J., Raynaud, C., Mohan, V. P., Lanéelle, M. A., Yu, K., Quémard, A., Smith, L., and Daffé, M. (2000) *Mol. Microbiol.* **36**, 630–637
- Dao, D. N., Sweeney, K., Hsu, T., Gurcha, S. S., Nascimento, I. P., Roshesky, D., Besra, G. S., Chan, J., Porcelli, S. A., and Jacobs, W. R. (2008) *PLoS Pathog.* **4**, e1000081
- Peyron, P., Vaubourgeix, J., Poquet, Y., Levillain, F., Botanch, C., Bardou, F., Daffé, M., Emile, J. F., Marchou, B., Cardona, P. J., de Chastellier, C., and Altare, F. (2008) *PLoS Pathog.* **4**, e1000204
- Dinadayala, P., Laval, F., Raynaud, C., Lemassu, A., Laneelle, M. A., Laneelle, G., and Daffe, M. (2003) *J. Biol. Chem.* **278**, 7310–7319
- Barry, C. E., 3rd, Lee, R. E., Mdluli, K., Sampson, A. E., Schroeder, B. G., Slayden, R. A., and Yuan, Y. (1998) *Prog. Lipid Res.* **37**, 143–179

- Alahari, A., Trivelli, X., Guéardel, Y., Dover, L. G., Besra, G. S., Sacchettini, J. C., Reynolds, R. C., Coxon, G. D., and Kremer, L. (2007) *PLoS ONE* **2**, e1343
- Yuan, Y., Mead, D., Schroeder, B. G., Zhu, Y., and Barry, C. E., 3rd (1998) *J. Biol. Chem.* **273**, 21282–21290
- Wang, A. Y., Grogan, D. W., and Cronan, J. E., Jr. (1992) *Biochemistry* **31**, 11020–11028
- Smith, D. D., Jr., and Norton, S. J. (1980) *Biochem. Biophys. Res. Commun.* **94**, 1458–1462
- Guianvarc'h, D., Guangqi, E., Drujon, T., Rey, C., Wang, Q., and Ploux, O. (2008) *Biochim. Biophys. Acta* **1784**, 1652–1658
- Boissier, F., Bardou, F., Guillet, V., Uttenweiler-Joseph, S., Daffé, M., Quémard, A., and Mourey, L. (2006) *J. Biol. Chem.* **281**, 4434–4445
- Lacave, C., Quémard, A., and Lanéelle, G. (1990) *Biochim. Biophys. Acta* **1045**, 58–68
- Daffé, M., Lanéelle, M. A., Asselineau, C., Levy-Frebault, V., and David, H. (1983) *Ann. Microbiol.* **134**, 241–256
- Laval, F., Haïtes, R., Movahedzadeh, F., Lemassu, A., Wong, C. Y., Stoker, N., Billman-Jacobe, H., and Daffé, M. (2008) *J. Biol. Chem.* **283**, 1419–1427
- Hansen, M. B., Nielsen, S. E., and Berg, K. (1989) *J. Immunol. Methods* **119**, 203–210
- Gomez-Flores, R., Gupta, S., Tamez-Guerra, R., and Mehta, R. T. (1995) *J. Clin. Microbiol.* **33**, 1842–1846
- Sankar, M. M., Gopinath, K., Singla, R., and Singh, S. (2008) *Ann. Clin. Microbiol. Antimicrob.* **7**, 15
- Collaborative Computational Project Number 4 (1994) *Acta Crystallogr. D Biol. Crystallogr.* **50**, 760–763
- Potterton, E., Briggs, P., Turkenburg, M., and Dodson, E. (2003) *Acta Crystallogr. D Biol. Crystallogr.* **59**, 1131–1137
- Leslie, A. G. W. (1987) in *Proceedings of the Daresbury Study Weekend: Computational Aspects of Protein Crystal Data Analysis* (Helliwell, J. R., Machin, P. A., and Papiz, M. Z., eds), pp. 39–50, Science and Engineering Research Council, Daresbury Laboratory, Warrington, UK
- Evans, P. R. (1993) in *Proceedings of the CCP4 Study Weekend: Data Collection and Processing* (Sawyer, L., Issacs, N., and Burley, S., eds) pp. 114–122, Science and Engineering Research Council, Daresbury Laboratory, Warrington, UK
- Read, R. J. (1986) *Acta Crystallogr. A* **42**, 140–149
- Emsley, P., and Cowtan, K. (2004) *Acta Crystallogr. D Biol. Crystallogr.* **60**, 2126–2132
- Murshudov, G. N., Vagin, A. A., and Dodson, E. J. (1997) *Acta Crystallogr. D Biol. Crystallogr.* **53**, 240–255
- Perrakis, A., Sixma, T. K., Wilson, K. S., and Lamzin, V. S. (1997) *Acta Crystallogr. D Biol. Crystallogr.* **53**, 448–455
- Kleywegt, G. J. (2007) *Acta Crystallogr. D Biol. Crystallogr.* **63**, 94–100
- Schüttelkopf, A. W., and van Aalten, D. M. (2004) *Acta Crystallogr. D Biol. Crystallogr.* **60**, 1355–1363
- Winn, M. D., Isupov, M. N., and Murshudov, G. N. (2001) *Acta Crystallogr. D Biol. Crystallogr.* **57**, 122–133
- McDonald, I. K., and Thornton, J. M. (1994) *J. Mol. Biol.* **238**, 777–793
- DeLano, W. L. (2002) *The PyMOL Molecular Graphics System*, DeLano Scientific, San Carlos, CA
- Sacchettini, J. C., Rubin, E. J., and Freundlich, J. S. (2008) *Nat. Rev. Microbiol.* **6**, 41–52
- Laskowski, R. A., MacArthur, M. W., Moss, D. S., and Thornton, J. M. (1993) *J. Appl. Crystallogr.* **26**, 283–291
- Huang, C. C., Smith, C. V., Glickman, M. S., Jacobs, W. R., Jr., and Sacchettini, J. C. (2002) *J. Biol. Chem.* **277**, 11559–11569
- McCammon, M. T., and Parks, L. W. (1981) *J. Bacteriol.* **145**, 106–112
- Zheng, S., Hausmann, S., Liu, Q., Ghosh, A., Schwer, B., Lima, C. D., and Shuman, S. (2006) *J. Biol. Chem.* **281**, 35904–35913
- Osborne, T. C., Obianyo, O., Zhang, X., Cheng, X., and Thompson, P. R. (2007) *Biochemistry* **46**, 13370–13381
- Rao, V., Fujiwara, N., Porcelli, S. A., and Glickman, M. S. (2005) *J. Exp. Med.* **201**, 535–543
- Freire, E. (2008) *Drug Discov. Today* **13**, 869–874
- Carr, R. A., Congreve, M., Murray, C. W., and Rees, D. C. (2005) *Drug Discov. Today* **10**, 987–992

Figure S1

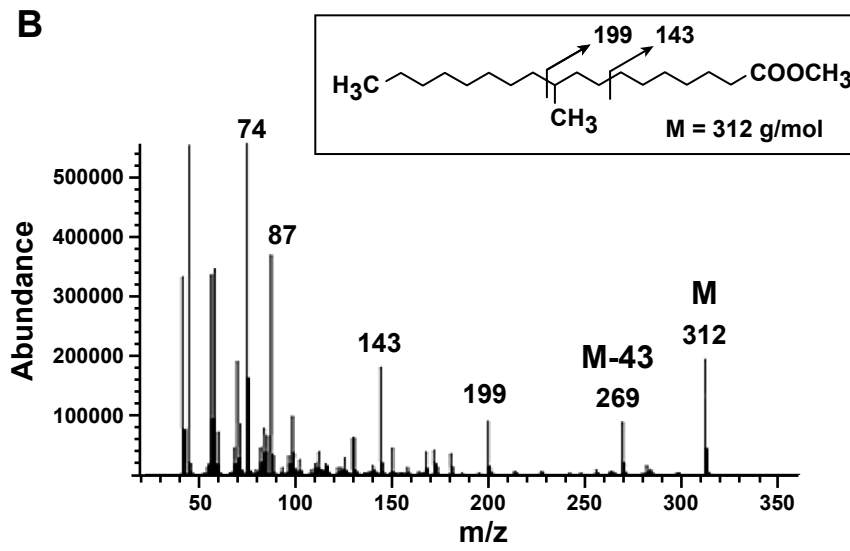
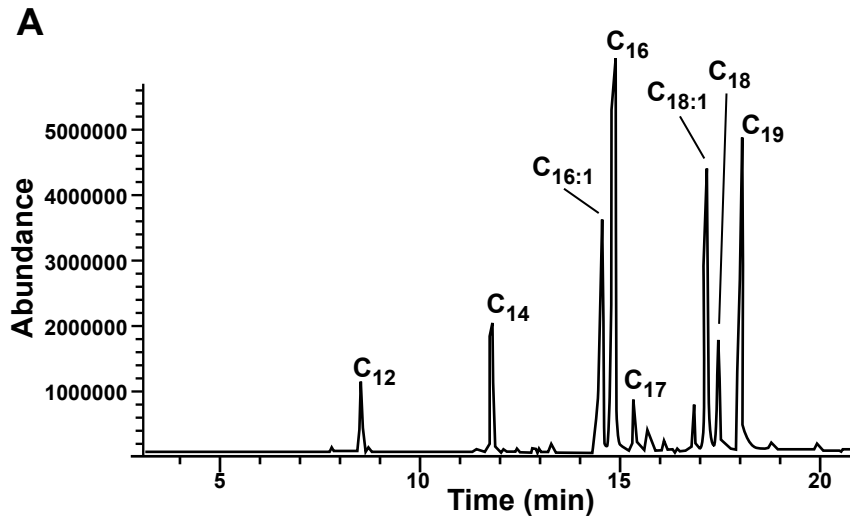


Figure S2

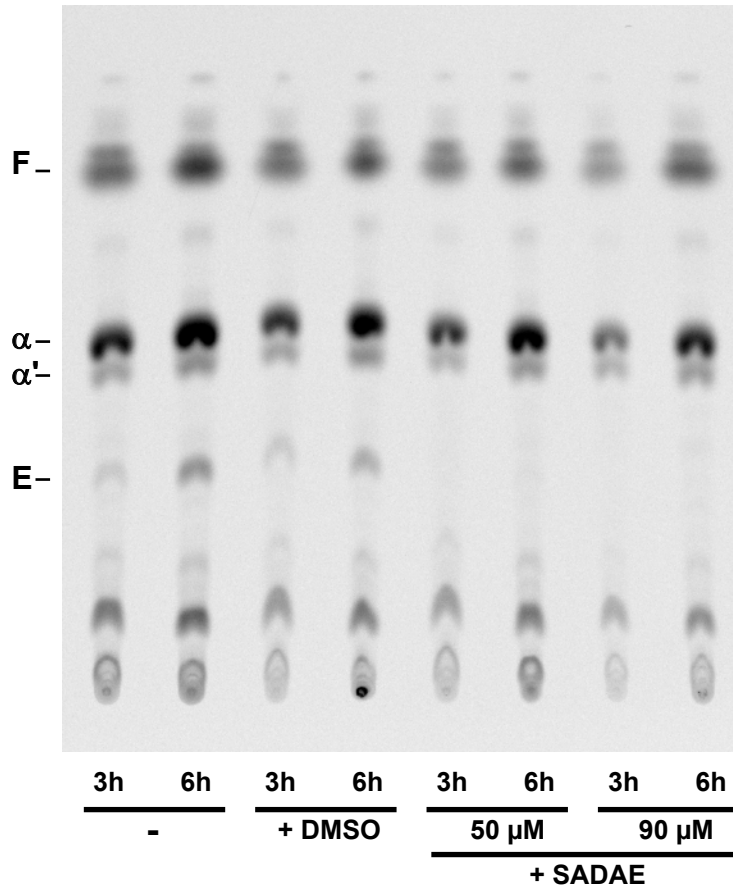


Figure S3

